SCIENCE CHINA
Information Sciences

• LETTER •

December 2019, Vol. 62 229401:1–229401:3
https://doi.org/10.1007/s11432-019-9894-0

Investigation of NbO_x-based volatile switching device with self-rectifying characteristics

Yichen FANG, Zongwei WANG, Caidie CHENG, Zhizhen YU, Teng ZHANG, Yuchao YANG, Yimao CAI* & Ru HUANG

Key Laboratory of Microelectronic Devices and Circuits (MOE), Institute of Microelectronics, Peking University, Beijing 100871*, China*

Received 18 March 2019/Revised 30 April 2019/Accepted 10 May 2019/Published online 8 November 2019

Citation Fang Y C, Wang Z W, Cheng C D, et al. Investigation of NbO_x-based volatile switching device with self-rectifying characteristics. Sci China Inf Sci, 2019, 62(12): 229401, https://doi.org/10.1007/s11432-019-9894-0

Dear editor,

Resistive random access memory (RRAM), one of the most promising emerging non-volatile memory technologies, has been extensively investigated by researchers from both academia and industry due to its fast speed and excellent scalability for storage class memory (SCM) [1–3]. To achieve large-scale integration in an RRAM array, each cell needs to contain a nonlinear device to eliminate the sneak path which may lead to false program and read-margin narrowing [2, 3]. Usually, transistors or selectors are serially connected to RRAM cells to act as the selective elements. Though effective, transistors will consume more area which undermines the scalability potential while some nonlinear devices may demand either non-conventional material or multi-layer-film controllability during fabrication processes [2, 3]. Recently, researchers have shown interest in threshold-switching selectors without additional area or processes. Niobium dioxide, one type of the insulator-metal transition (IMT) materials, has shown its potential as selector. While questions have been raised about further optimization of fabrication process, the electroforming operation to activate IMT and high leakage current for IMT-based selector devices [4–6]. Several attempts have been made to employ niobium oxide as nonlinear layer to avoid the initialization of IMT materials and its consequential challenges [5, 6]. However, the understanding of niobium oxide as nonlinear layer and its underlying mechanism remain elusive and further discussions are needed.

We present a comprehensive investigation on the role of niobium oxide as nonlinear layer and its interaction with electrode material. By using nondestructive characterization methods such as electrical and high-temperature test, the origin of the volatile switching characteristics with self-rectifying feature and the conductive mechanism were experimentally examined and discussed, which provides substantial insights into the mechanism of niobium-oxide material as nonlinear material and contributes to the advancement of large-scale integration of selector and RRAM.

Experiment details. The device fabrication process are as follows. Silicon dioxide layer was deposited by chemical vapor deposition (CVD) as electrical isolation. Gold bottom electrode (40 nm) with Titanium adhesion layer (2 nm) were deposited by electron beam evaporation and patterned by lift-off. Niobium oxide film with thickness around 12 nm was sputtered. Then, the sample was processed by oxygen plasma to complete further oxidization. Finally, Palladium of 50 nm was sputtered and patterned by lift-off as the top electrode. During the test, the top electrode was connected to the voltage source, while the bottom electrode was grounded. The electrical test was conducted through Agilent B1500A.

* Corresponding author (email: caiyimao@pku.edu.cn)

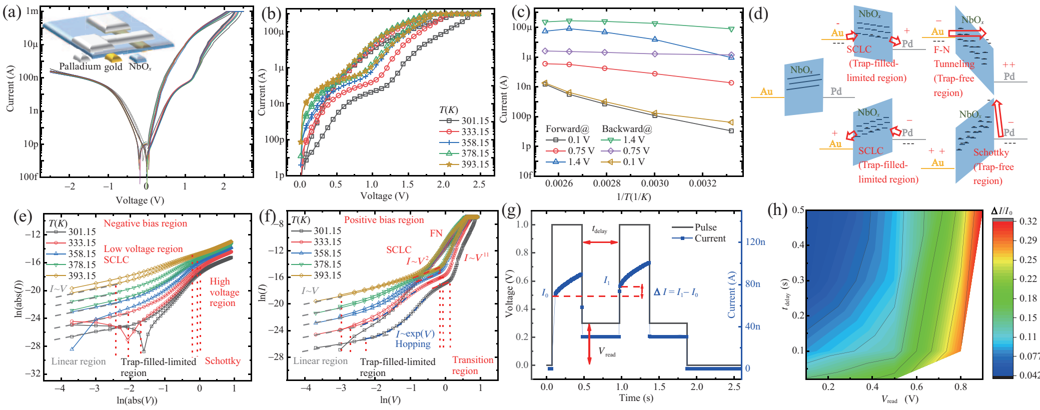

Figure 1 (Color online) (a) DC sweeping curves of fifteen Au/NbO_x/Pd devices. The inset includes a schematic of the device structure. (b) The positive bias curves of the device under heating test ranging from room temperature to 120°C. (c) is extracted from several devices and a current versus reciprocal temperature is plotted. (d) The band diagrams helps to illustrate the conduction mechanisms of the device. Natural logarithm of voltage versus natural logarithm of current for SCLC fitting of negative bias region (e) and positive bias region (f). In (e) and (f), grey dashed lines present curves in linear region. Red dashed lines present curves obeying child's law in SCLC. The linear region, trap-filled-limited region and trap-free region are divided by vertical dotted lines. (g) An example shows the applied pulse waveform, the current curve and the delta current from two sequential pulses. (h) The color contour map summarizes the results of the pulse test of volatility.

Results and discussions. The DC characteristics of the devices under room temperature are presented in Figure 1(a). It is worth noticing that the devices do not need the forming operation to initialize, which is totally different from IMT devices. From the DC curves, it can be seen that the devices present self-rectifying characteristics. Specifically, the current under positive bias is significantly larger than the current under negative bias when the absolute value of applied voltage exceeds 1 V. More interestingly, the positively biased devices present volatile switching behavior, which shows large hysteresis in DC sweep mode, and 1 mA compliance current is set in case of breakdown. Though the results in Figure 1(a) were collected from fifteen devices, they present minor device-to-device variation which may attribute to the integrity of NbO_x film. In addition, the endurance of the device was tested to be larger than 10^6 with superb uniformity in supplements, indicating a fine control over cycle-to-cycle variation. The dependence of switching characteristics on area is negligible, indicating that the conductive path may be dominated by local defect sites.

To comprehensively analyze the device performance, high temperature test were performed by ranging the temperature of probe station from room temperature to 120°C. The results are illustrated in Figure 1(b) and (c), from which several trends can be concluded. Both the positively and the negatively sweeping curves are generally sensitive to temperature, but it is slightly complicate for positively sweeping side. It is noticed that the positive bias around 1 V divides the curve into different ranges. The current in relatively low-voltage range tends to be more dependent on temperature than the high-voltage range current. The current from the sweeping-back curve tends to be less dependent on temperature than the one from the forward-sweeping part.

In order to understand the unique characteristics of the device, it is necessary to analyze the mechanism of current transportation. According to the different thermal performance of the device current, we attempt to discuss the performance into four regions, which is divided by the polarity and the intensity of the bias. Firstly, the negatively biased curves of high voltage region were found to be in accordance with the Schottky mechanism with the fitting relation of $\ln(\text{abs}(I))$ vs. $\text{abs}(V^{1/2})$. Not only the curves but also the dependence of their slopes on temperature are correctly fitted, as is shown in Figure 1(e). Secondly, the positively backward biased curves of high voltage region could be fitted with the Fowler-Nordheim tunneling with the relation of $\ln(I/V^2)$ vs. $1/V$, which typically occurs in the high voltage region and presents weak temperature dependence. In addition, the curves in this region, especially the relatively low temperature ones, still present weak temperature dependence, which may be attributed to the extending influence of the component from low voltage region. The positively biased curves in the forward direction, however, present significant temperature dependence in Figure 1(e) and (f), which excludes F-N tunneling mechanism. The low voltage region, including both the positively and the negatively biased parts, could fit with the space charge limited current (SCLC) mechanism instead of mechanisms such as Schottky, F-N tunneling and Pool-Frenkle. The current curves fit well with the linear region, the trap filled limited region and the trap free region, as is predicted in the SCLC mechanism. Yet, there are still differences between traditional SCLC and our case, which are listed below.

For negative bias, the current experiences a transition from the trap-filled-limited region to Schottky emission region, which is strongly supported by the fitting results mentioned above. For positive bias, the back sweeping current presents F-N tunneling mechanism which is almost thermal independent. The forward sweeping current complies with SCLC child's law ($I \sim V^2$) after the trap-filled-Region. Then the current increases abruptly and reaches the preset compliance in case of breakdown. The difference between positive and negative bias after trap-filled-limited region is mainly ascribed to the difficulty of electron injection caused by the different barrier height of the palladium side and the gold side. It leads to the domination of Schottky during the negative high voltage region, while the transition region appears and current grows sharply during the positive high voltage region. The band diagrams and corresponding conduction mechanisms are shown in Figure 1(d), which helps to illustrate this difference. For positive forward bias, the current experiences trap-filled-limited region, during which the curves can be partly fitted by hopping. After this region, the current grows sharply with increasing voltage. The first reason is that injected electrons are sufficient to fill most traps, leading to the trap-free transition region predicted by SCLC. The second reason is that the niobium oxide contains certain niobium dioxide, in which the IMT happens and leads to the abrupt current increase.

With the analysis of the conduction mechanisms, the volatile switching under positive bias region can be understood. As is shown in Figure 1(g), the current increases gradually with voltage. This agrees well with the scheme in SCLC when the traps are filled gradually. The filled traps do not release the electron right after the voltage becomes lower. Instead, they need a period of time to be released. To measure the time for this relaxation period, a series of pulse with several test schemes were performed as shown in Figure 1(g). After applying the first pulse, a second pulse with the same parameters was applied with various amplitudes of the reading voltage to characterize the relaxation. Another scheme realized by tuning the delay between the first and the second pulse as shown. By varying both the delay and the amplitude of reading voltage, we obtain the delta current data and summarize them in Figure 1(h). It can be concluded that before the reading voltage reaches around 0.5 V, the device needs about 80 ms to relax. When the reading voltage comes to be higher than 0.5 V, the device does not relax any more, which may be a rough reflection of the energy gap between the trap-energy level and the Fermi level of gold electrode. By calculating from relaxation time of 80 ms according to the phonon tunneling formula in [7], we can obtain the trap barrier about 0.3 V, which implies a coincidence of the two phenomena.

Conclusion. The niobium oxide based nonlinear devices were fabricated and analyzed. The electrical tests present good control over device-to-device variation and stable endurance more than 10^6. The conduction mechanism was comprehensively discussed. The low-voltage region relates to SCLC, while Schottky and F-N tunneling are responsible for negative and positive high-voltage region respectively. Consequently, the volatile switching may originate from the capture and release of electrons by traps in SCLC mechanism, and this relaxation phenomenon is evaluated quantitatively.

Acknowledgements This work was supported by National Natural Science Foundation of China (Grant Nos. 61834001, 61574007, 61421005) and 111 Project (Grant No. B18001).

Supporting information Appendix A. The supporting information is available online at info.scichina.com and link.springer.com. The supporting materials are published as submitted, without typesetting or editing. The responsibility for scientific accuracy and content remains entirely with the authors.

References

1 Hudec B, Hsu C W, Wang I T, et al. 3D resistive RAM cell design for high-density storage class memory — a review. Sci China Inf Sci, 2016, 59: 061403
2 Zhao X L, Wang R, Xiao X H, et al. Flexible cation-based threshold selector for resistive switching memory integration. Sci China Inf Sci, 2018, 61: 060413
3 Cui X L, Zhang Q, Cui X X, et al. Testing of 1TnR RRAM array with sneak path technique. Sci China Inf Sci, 2017, 60: 029402
4 Park J, Cha E, Karpov I, et al. Dynamics of electroforming and electrically driven insulator-metal transition in NbO_x selector. Appl Phys Lett, 2016, 108: 232101
5 Kim K M, Zhang J, Graves C, et al. Low-power, self-rectifying, and forming-free memristor with an asymmetric programing voltage for a high-density crossbar application. Nano Lett, 2016, 16: 6724–6732
6 Park J H, Jeon D S, Kim T G. Ti-doped GaO_x resistive switching memory with self-rectifying behavior by using NbO_x/Pt bilayers. ACS Appl Mater Interface, 2017, 9: 43336–43342
7 Krause H. Tunnel hopping current and trap filling in insulating layers. Phys Stat Sol, 1979, 52: 565–575